

# Expression profile, molecular functions, and prognostic significance of miRNAs in primary colorectal cancer stem cells

Chuan-Wen Fan<sup>1,2,3,4</sup>, Ran Lu<sup>4</sup>, Chao Fang<sup>1</sup>, Xue-Li Zhang<sup>5</sup>, Zhao-Ying Lv<sup>1</sup>, Yuan Li<sup>1</sup>, Hong Zhang<sup>5</sup>, Zong-Guang Zhou<sup>1,8</sup>, Xian-Ming Mo<sup>4</sup>, Xiao-Feng Sun<sup>3</sup>

<sup>1</sup>Institute of Digestive Surgery, Sichuan University, and Department of Gastrointestinal Surgery, West China Hospital, West China School of Medicine, Sichuan University, Chengdu, China

<sup>2</sup>Department of Gastrointestinal Surgery and Breast and Thyroid Surgery, Minimally Invasive Surgery, West China Fourth Hospital, Sichuan University, Chengdu, China

<sup>3</sup>Department of Oncology and Department of Biomedical and Clinical Sciences, Linköping University, Linköping, Sweden

<sup>4</sup>Laboratory of Stem Cell Biology, West China Hospital, Sichuan University, Chengdu, China

<sup>5</sup>School of Medicine, Institute of Medical Sciences, Örebro University, Örebro, Sweden

**Correspondence to:** Zong-Guang Zhou, Xian-Ming Mo, Xiao-Feng Sun; **email:** [zhou767@163.com](mailto:zhou767@163.com), [xmingmo@scu.edu.cn](mailto:xmingmo@scu.edu.cn), [xiao-feng.sun@liu.se](mailto:xiao-feng.sun@liu.se)

**Keywords:** miRNAs, cancer stem cells, progression, prognosis, colorectal cancer

**Received:** October 19, 2020

**Accepted:** March 13, 2021

**Published:** April 1, 2021

**Copyright:** © 2021 Fan et al. This is an open access article distributed under the terms of the [Creative Commons Attribution License](https://creativecommons.org/licenses/by/3.0/) (CC BY 3.0), which permits unrestricted use, distribution, and reproduction in any medium, provided the original author and source are credited.

## ABSTRACT

MicroRNAs (miRNAs) are known to drive the pathogenesis of colorectal cancer (CRC) via the regulation of cancer stem cells (CSCs). We studied the miRNA expression profile of primary CSCs isolated from patients with CRC (pCRCSCs). Compared to pCRCSC-derived differentiated cells, 98 differentially expressed miRNAs were identified in pCRCSCs. Target genes encoding pCRCSC-related miRNAs were identified using a combination of miRNA target databases and miRNA-mRNA regulatory networks from the same patient. The pCRCSC-related miRNA target genes were associated with pathways contributing to malignant phenotypes, including I-kappa B kinase/NF-kappa B signaling, signal transduction by p53 class mediator, Ras signaling, and cGMP-PKG signaling. The pCRCSC-related miRNA expression signature was independently associated with poor overall survival in both the training and validation cohorts. We have thus identified several pCRCSC-related miRNAs with oncogenic potential that could serve as prognostic biomarkers for CRC.

## INTRODUCTION

Colorectal cancer (CRC) is one of the leading causes of cancer-related death worldwide due in large part to its strong recurrence and metastatic potentials [1]. Cancer stem cells (CSCs), a subset of cancer cells, are characterized by sphere formation, self-renewal, and multi-lineage differentiation, and contribute to cancer initiation and metastasis and resistance to chemotherapy, radiotherapy, and targeted therapy in various cancer types, including CRC [2]. We previously isolated and identified primary rectal CSCs and

showed their characteristic phenotypes [3]. Further studies indicated that these primary CSCs can transdifferentiate into endothelial cells and neurons to support the growth of CRC cells [4, 5]. Compared with CSCs derived from cancer cell lines, primary CSCs are practically more relevant and reflect the actual tumor conditions in cancer patients [6]. However, a detailed understanding of malignant characteristics of primary CSCs isolated from patients with CRC (pCRCSCs) and the underlying molecular mechanisms of development of CSCs is required to mimic the CSC characteristics *in vivo*.

MiRNAs are small non-coding RNAs of approximately 20 to 25 nucleotides in length that regulate the expression of more than 60% of human genes. Recent findings have implicated several miRNAs, such as miR-21 [7], miR-27a [8], miR-31 [9], miR-137 [10], miR-146a [11], miR-148a [12], miR-195-5p [13], miR-196b-5p [14], miR-199a/b [15], miR-215 [16], miR-372/373 [17], and miR-1246 [18], in the regulation of CSC characteristics including self-renewal and differentiation [19, 20]. MiRNAs execute these functions by targeting the genes of several essential signaling pathways, such as Wnt/ $\beta$ -catenin and Notch, associated with the maintenance, growth, and function of CSCs [21]. However, a global miRNA expression profile of CRCSCs, especially of pCRCSCs is still unavailable. Moreover, CSC-related signaling pathways do not function in isolation but as a coordinated network [22, 23], implying that CSC phenotypes are an output of several signaling networks. Similarly, a single miRNA can target multiple genes and signaling pathways. Therefore, a single agent targeting the rare CSC subpopulations, although can reduce the tumor volume, cannot eliminate the tumor, highlighting the need to elucidate the regulatory network of pCRCSCs.

We performed a comprehensive global miRNA expression analysis of differentiated pCRCSCs to identify differentially expressed miRNAs. Further, molecular functions of differentially expressed miRNAs were annotated and their prognostic significance in patients with CRC was analyzed. The study design is shown in Figure 1.

## RESULTS

### Expression profiles of miRNAs in pCRCSCs and their corresponding pCRCSC-derived differentiated cells

To isolate colon CSCs, primary CSCs from patients with CRC were enriched in serum-free medium supplemented with epidermal growth factor (EGF) and basic fibroblast growth factor (bFGF). After 3 to 4 weeks, a small fraction of tumor cells formed spheres (Figure 2A). Next, the serum-free CSC medium was replaced with 20% fetal bovine serum (FBS)-containing medium to differentiate the spheres [3, 24]. The spherical cells in the culture gradually aggregated into clusters of polygonal cells and exhibited typical epithelial-like tumor cell morphology (Figure 2A).

To study tumorigenesis between the expanded pCRCSCs and pCRCSC-derived differentiated cells (termed differentiated pCRCSCs in the following text), both cell types were injected into immunodeficient mice and xenograft growth was assessed. Compared to

differentiated pCRCSCs, pCRCSCs formed bigger tumor masses, with a faster growth (Figure 2B, 2C). In addition, mice-bearing pCRCSCs lost more weight than those bearing differentiated pCRCSCs (Figure 2D).

To further investigate the difference in the potential miRNAs regulating tumorigenesis between pCRCSCs and differentiated pCRCSCs, a global miRNA expression profile analysis was performed in three pCRCSCs and paired differentiated pCRCSCs including one primary CSC isolated from a patient with CRC and two previously enriched primary CSCs isolated from patients with rectal cancer [3]. In total, 98 differentially expressed miRNAs were identified between pCRCSCs and differentiated pCRCSCs, of which 50 were up-regulated and 48 were downregulated (Figure 2E and Supplementary Table 1).

### Identification of target genes and regulatory network of pCRCSC-related miRNAs

Because miRNAs function by binding to their specific target genes, we first used miRWalk, TargetScan, and miRDB databases to predict target genes for all 98 differentially expressed miRNAs in pCRCSCs. Only genes that were commonly predicted by all three databases were used as putative target genes. In total, 18,792 potential target genes were identified (Supplementary Table 2). To more accurately identify the miRNA targets, we analyzed the miRNA and mRNA differential expression profile datasets of the same patients using the TCGA database. We identified 745 miRNAs and 5,558 mRNAs ( $|\log_2 \text{FC}| > 2$ ,  $p < 0.05$ ) that were differentially expressed in normal and CRC samples (Supplementary Tables 3, 4). The negatively regulated miRNA/mRNA pairs (miRNA upregulated/mRNA downregulated or miRNA downregulated/mRNA upregulated) were obtained and intersected with predictive target mRNAs in the database. The 1,103 miRNA/mRNA pairs were identified, including 35 miRNAs and 870 mRNAs, were believed to be related to miRNA-regulated target genes in pCRCSCs (Supplementary Table 5). The miRNA–mRNA regulatory network is shown in Figure 3.

### Relevant biological functions and pathways affected by pCRCSC-related miRNAs

To assess the biological functions of pCRCSC-related miRNAs, the functions and pathways of targeted genes of pCRCSC-related miRNAs were analyzed using the DAVID database. In total, 868 genes were found enriched in 68 gene ontology (GO) terms including 23 biological processes, 31 cell components, and 14 molecular functions (Figure 4A–4C and Supplementary Table 6). The enriched biological processes included

mRNA splicing regulation, I-kappa B kinase/NF-kappa B signaling, and signal transduction by p53 class mediator, which were linked to malignant features of CSCs. Protein binding, poly(A) RNA binding, nucleotide binding, and ubiquitin protein ligase binding were highly enriched molecular functions.

The pCRCSC-related miRNAs were enriched in several cancer-related pathways, including Ras signaling pathway, actin cytoskeleton regulatory pathways, cGMP–PKG signaling pathway, and spliceosome pathways, which correlated with the malignant phenotype of cancer cells (Figure 4D and Supplementary Table 7).

Because pCRCSC-related miRNA targets were predicted by bioinformatics, certain potential targets involved in the key pathways were selected and examined by quantitative reverse transcription-polymerase chain reaction (RT-qPCR) for validation. The expression of selected potential targets was congruent with the results of predictive miRNA target databases, validating the involvement of predictive miRNA-related signaling pathways in CRC (Figure 4E, 4F).

### Identification of potential prognostic miRNA signatures for CRC

To evaluate the prognostic function of pCRCSC-related miRNAs in patients with CRC, we first randomly grouped the TCGA–COREAD data into training and validation cohorts (Supplementary Table 8). The prognostic significance of 35 functionally annotated pCRCSC-related miRNAs was further investigated using univariate Cox proportional hazards regression analyses in the training cohort (Supplementary Table 9).

Prognosis-related miRNAs were subsequently selected for multivariate Cox proportional hazards regression analyses. Finally, two pCRCSC-related miRNAs (miR-664b-3p [risky miRNA] and miR-200c-5p [protective]) were confirmed as independent prognostic miRNAs of patients with CRC in the training cohort (Supplementary Table 10). To facilitate the use of pCRCSC-related miRNAs as prognostic markers in routine clinical practice, we next developed a formula to calculate the risk score of overall survival (OS) using the Cox proportional hazard regression model for each patient based on the expression of two pCRCSC-related miRNAs, where risk score =  $(0.384 \times \text{expression of miR-664b-3p}) - (0.270 \times \text{expression of miR-200c-5p})$ .

### Clinical significance of prognostic miRNA signature in CRC patients

The patients were classified into low- and high-risk groups in the training and validation cohorts using X-tile plots to generate the optimal cut-off score (Supplementary Figure 1). Correlation analysis of clinicopathological characteristics of patients between high- and low-risk groups revealed remarkable differences only in the stage and survival status of patients in both training and validation cohorts (Table 1). In addition, as shown in Figure 5A, 5B, the distribution of miRNA-based risk scores, OS time, OS status, and the expression of two pCRCSC-related miRNAs in the training and validation cohorts showed that high-risk patients were associated with higher mortality than low-risk patients. The heat map revealed that the risky miR-664b-3p was highly expressed in high-risk patients, whereas protective miR-200c-5p was highly expressed in low-risk patients in both training and validation cohorts (Figure 5A, 5B).

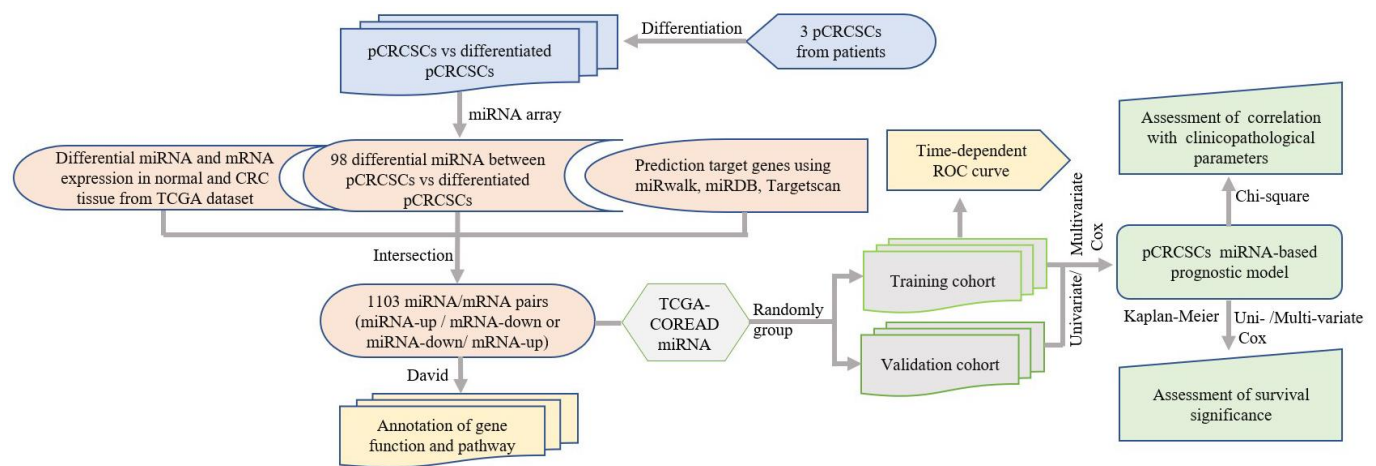


**Figure 1. Study design.** pCRCSCs: primary colorectal cancer stem cells.

Survival analyses showed that the 5-year OS was 56.3% (95% confidence interval [CI]: 42.7–74.2) for high-risk patients and 71.5% (95% CI: 57.8–88.3) for low-risk patients (Figure 5C;  $p = 0.003$ ) after assessing the prognostic accuracy of two miRNA-based classifiers with time-dependent ROC analysis at varying follow-up times (Supplementary Figure 2A, 2B). The classifier universality of two pCRCSC-related miRNAs in different populations was confirmed by applying it to the validation cohort, thereby classifying 110 (41%) patients as high risk and 156 (59%) patients as low risk. Five-year OS was 28.1% (95% CI: 14.6–54.1) for

high-risk patients and 71.4% (95% CI: 59.3–81.6) for low-risk patients (Figure 5D;  $p < 0.001$ ).

### Assessment of independent prognostic significance of miRNA signature in CRC patients

To further assess whether the pCRCSC-related miRNA signature could independently predict OS in patients with CRC, both univariate and multivariate Cox regression analyses were performed by adjusting for gender, age, tumor location, stage, microsatellite instability (MSI) status, and adjuvant

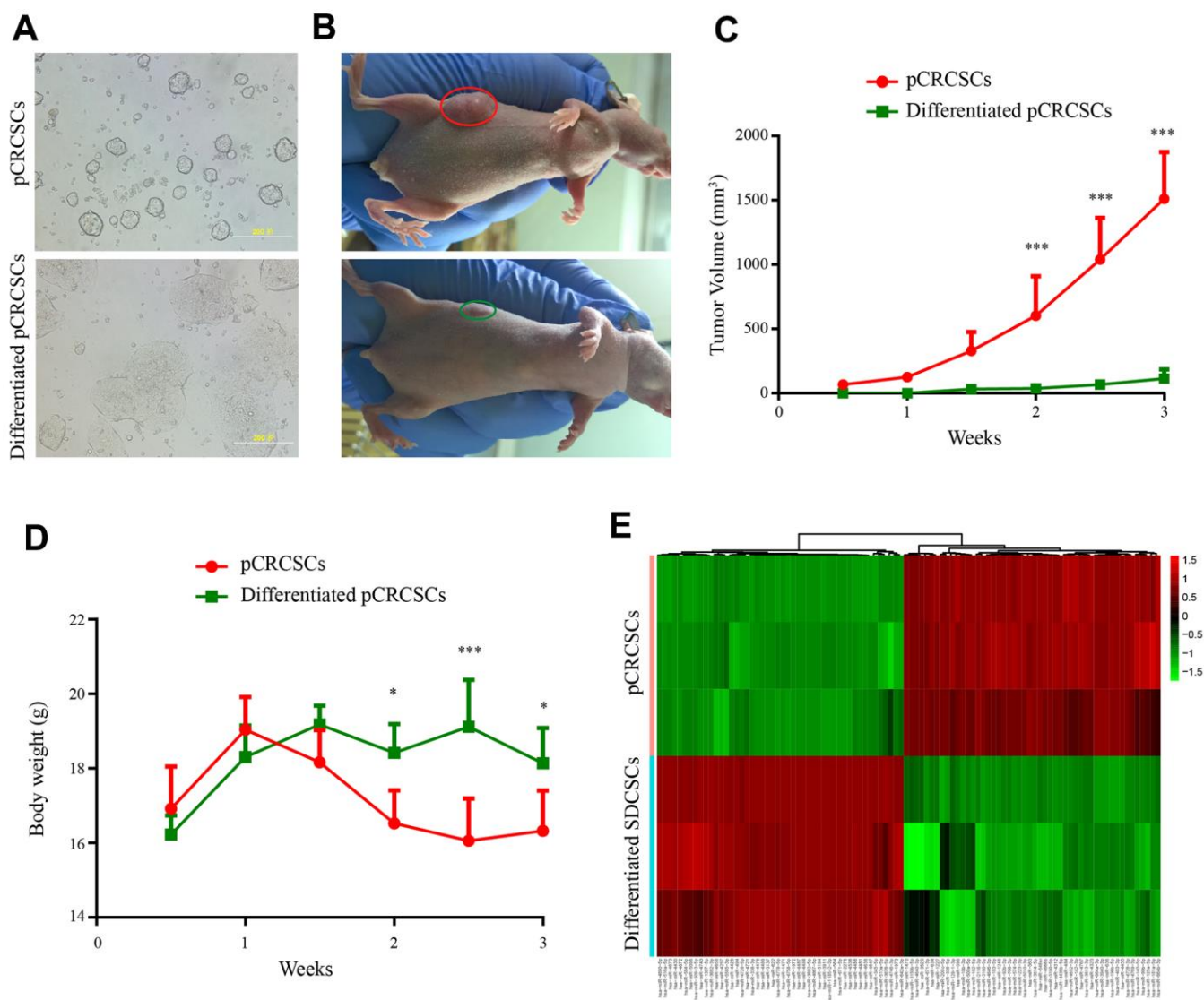


**Figure 2. Differential tumorigenic capacity and distinct expression profiles of miRNAs between pCRCSCs and pCRCSC-derived differentiated cells.** (A) pCRCSCs generated from a human colon cancer sample and their corresponding differentiated pCRCSCs. Bars = 200  $\mu$ M. (B) A tumor-bearing nude mouse showing a large xenograft tumor from pCRCSCs (red oval) and a small tumor from pCRCSC-derived differentiated cells (green oval). (C) Tumor volume of the subcutaneous tumor generated from  $5 \times 10^5$  pCRCSCs and differentiated pCRCSCs. (D) Weight of tumor-bearing mice. Bars represent mean  $\pm$  standard deviation (SD) ( $n = 5$ , \* $p < 0.05$ , \*\*\* $p < 0.001$ ). (E) Heat map of differentially expressed miRNAs in pCRCSCs and pCRCSC-derived differentiated cells.



chemoradiotherapy as covariates. Univariate analyses revealed that the pCRCSC-related miRNA signature was significantly associated with OS (Supplementary Table 11; hazard ratio [HR] = 2.17,  $p = 0.015$ ). Moreover, the pCRCSC-related miRNA signature was significant, even after adjusting for other covariates in the training cohort (Figure 6A, HR = 2.30, 95% CI: 1.17–4.60,  $p = 0.016$ ). Similarly, the prognostic significance of pCRCSC-related miRNA signature with OS was validated in the validation cohort (Supplementary Table 12; HR = 3.71,  $p < 0.001$ ). Multivariate analyses revealed that the pCRCSC-related miRNA signature remained a powerful prognostic factor in the validation cohort after adjusting for other covariates (Figure 6B, HR = 3.93, 95% CI: 2.09–7.40,  $p < 0.001$ ).

## DISCUSSION

Tumor resistance to traditional chemotherapy and radiotherapy is partially attributed to CSCs and results in cancer recurrence and metastasis [25]. We have previously shown that CSCs from primary rectal adenocarcinoma have a strong tumorigenic capacity and are resistant to common therapeutic drugs used for treating patients with advanced or metastatic CRC [3]. In this study, we further evaluated the tumorigenesis of CSCs of primary colon adenocarcinoma that exhibited strong tumorigenic potential, indicating the common

malignant features of primary CSCs of both colon and rectal cancers.

Altered miRNA expression has been shown to contribute to the malignant behavior of CSCs [26]. A comprehensive analysis of the miRNA expression profile revealed 98 differentially expressed miRNAs in pCRCSCs, of which 50 were upregulated and 48 were downregulated. Some of these miRNAs, such as miRNA 200c [27, 28], miR-1246 [29], and miR-494 [30], are involved in the regulation of CSCs. For example, miR-1246 activates the Wnt/ $\beta$ -catenin pathway by inhibiting the expression of Axin-2 and GSK-3 $\beta$  to maintain the stemness of CSCs, including self-renewal, drug resistance, and tumorigenicity [29]. Similarly, miR-494 inhibits BMI-1 expression and prevents self-renewal of breast CSCs/progenitor cells [30]. Furthermore, miRNAs regulate four major signal transduction pathways that affect CSC characteristics: Wnt/ $\beta$ -catenin, BMI-1, Notch, and Hedgehog, and the corresponding pathways [8]. Therefore, we not only confirmed the potential significance of previously published miRNAs in CSCs but also identified certain novel miRNAs affecting the malignant features of pCRCSCs.

Pathway enrichment analysis revealed differentially expressed pCRCSC-related miRNAs to be enriched in I-kappa B kinase/NF-kappa B signaling, signal

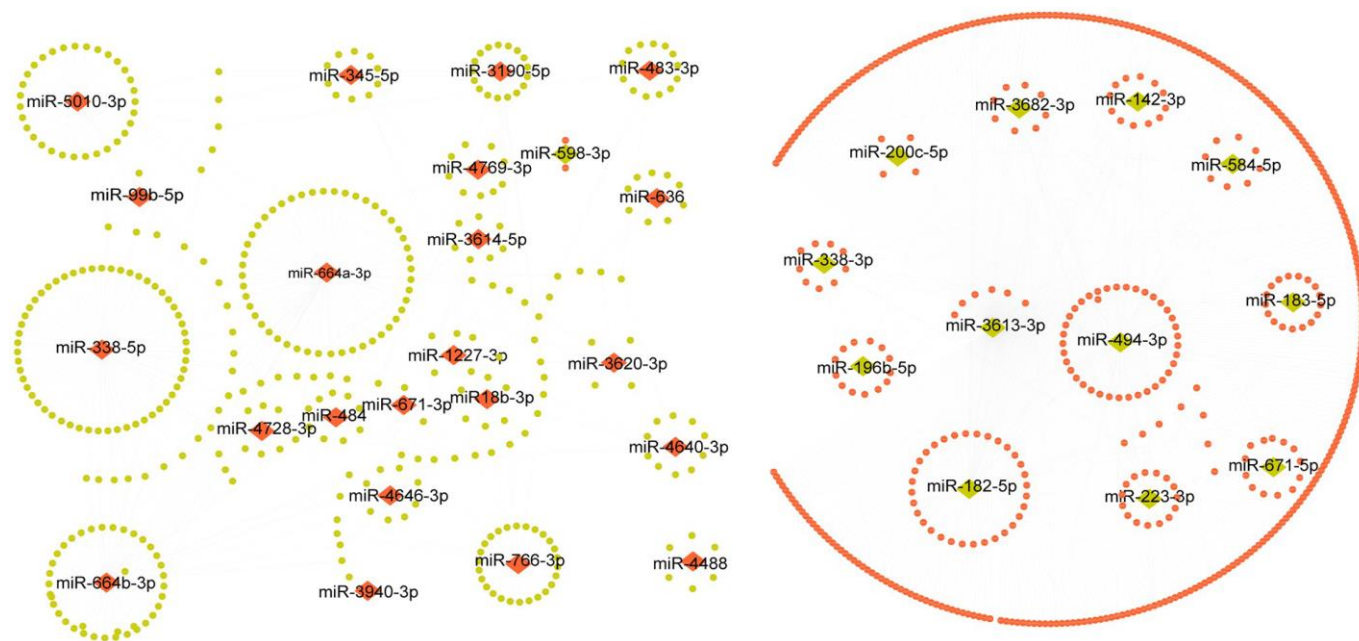


**Figure 3. The regulatory network of pCRCSC-related miRNAs.** Upregulated miRNAs are shown as red diamonds and the corresponding downregulated target genes in the TCGA database are shown as green ellipses. The downregulated miRNAs are shown as green diamonds and the corresponding upregulated target genes in the TCGA database are shown as red ellipses.

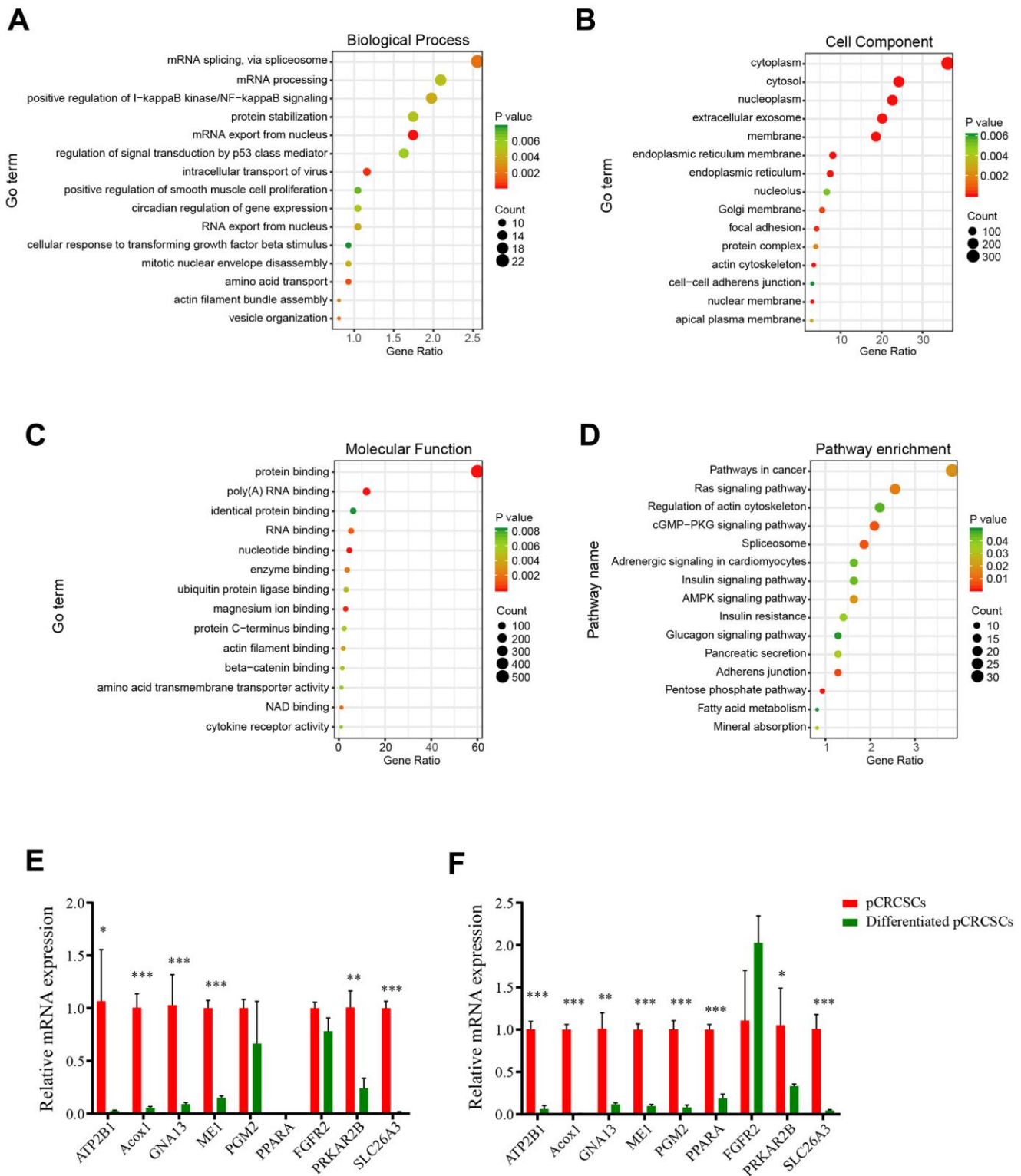


**Figure 4. The GO and KEGG pathways of pCRCSC-related miRNAs.** (A) The top 15 biological processes, (B) cell components, (C) molecular functions, and (D) the KEGG pathways of target genes based on the intersection of predicted downstream target genes and genes that negatively correlated with miRNA expression in the TCGA-COREAD dataset. (E) Nine potential target genes of pCRCSC-related miRNAs were validated by RT-qPCR in the primary CSCs derived from colon cancer and the corresponding differentiated cells. (F) Nine potential target genes of pCRCSC-related miRNAs were validated by RT-qPCR in the primary CSCs derived from rectal cancer and the corresponding differentiated cells. GAPDH was selected as the internal control. This experiment was repeated thrice. Bars represent mean  $\pm$  standard deviation (SD) ( $n = 3$ , \* $p < 0.05$ , \*\* $p < 0.01$ , \*\*\* $p < 0.001$ ).

**Table 1. Baseline characteristics of patients by miRNA assessment cohorts.**

Parameters	Training set			Validation set		
	Low risk	High risk	p value	Low risk	High risk	p value
<b>Gender</b>						
Female	67 (43.8)	56 (49.6)	0.351	73 (45.9)	53 (49.5)	0.562
Male	86 (56.2)	57 (50.4)		86 (54.1)	54 (50.5)	
<b>Age (years)</b>						
≤65	68 (44.4)	55 (48.7)	0.494	69 (43.4)	49 (45.8)	0.700
>65	85 (55.6)	58 (51.3)		90 (56.6)	58 (54.2)	
<b>Tumor location</b>						
RSCC	81 (52.9)	39 (34.5)	0.004	65 (40.9)	43 (40.2)	0.959
LSCRC	67 (43.8)	68 (60.2)		91 (57.2)	61 (57.0)	
NA	5 (3.3)	6 (5.3)		3 (1.9)	3 (2.8)	
<b>Stage</b>						
Stage I	31 (20.3)	12 (10.6)	<b>0.032</b>	35 (22.0)	15 (14.0)	<b>0.001</b>
Stage II/III	103 (67.3)	79 (69.9)		106 (66.7)	63 (58.9)	
Stage IV	15 (9.8)	20 (17.7)		15 (9.4)	28 (26.2)	
NA	4 (2.6)	2 (1.8)		3 (1.9)	1 (0.9)	
<b>MSI status</b>						
MSS	118 (77.1)	107 (94.7)	<0.001	133 (83.6)	100 (93.5)	0.069
MSI	35 (22.9)	6 (5.3)		21 (13.2)	7 (6.5)	
NA				5 (3.1)		
<b>Radiochemotherapy</b>						
No	90 (58.8)	58 (51.3)	0.224	109 (68.6)	58 (54.2)	0.018
Yes	63 (41.2)	55 (48.7)		50 (31.4)	49 (45.8)	
<b>Survival status</b>						
Alive	134 (87.6)	82 (72.6)	<b>0.002</b>	134 (84.3)	68 (63.6)	<b>&lt;0.001</b>
Dead	19 (12.4)	31 (27.4)		25 (15.7)	39 (36.4)	
<b>Recurrence</b>						
No	103 (67.3)	77 (68.1)	0.69	113 (71.1)	67 (62.6)	0.049
Yes	29 (19.0)	19 (16.8)		21 (13.2)	24 (22.4)	
NA	21 (13.7)	17 (15.0)		25 (15.7)	16 (15.0)	

Note: NA: Missing data; RSCC: right-sided colon cancer; LSCRC: left-sided colorectal cancer. Bold values indicate the statistical significance parameters in both training and validation sets (P<0.05).

transduction by p53 class mediator, Ras signaling pathway, actin cytoskeleton regulation, cGMP-PKG signaling pathway, and spliceosome pathways, which are known to correlate with the malignant phenotype of cancer cells [31–33]. Moreover, the majority of pathways reported to be related to pCRCSC-related miRNAs have functional implications in CSCs. For instance, p53 and Ras signaling pathways regulate stem cell differentiation and self-renewal [23, 34]. In addition, p53 regulates certain stem factors or miRNAs, including Bmi-1 and miR-34 [35]. Similarly, the NF-κB pathway has been implicated in inflammation, self-renewal, and maintenance and metastasis of CSCs [36]. Interestingly, a cross-talk among these CSC-related signaling pathways has been reported [22, 23, 37].

Further, univariate and multivariate Cox regression analyses revealed an association between pCRCSC-related miRNA expression and survival. MiR-664b-3p and miR-200c-5p were identified as independent prognostic biomarkers in patients with CRC. MiRNA-200c is a well-studied miRNA in a variety of tumors, including CRC, due to its involvement in epithelial-mesenchymal transition and drug resistance [28]. In addition, miRNA-200c is associated with patient clinicopathology and prognostic significance in certain specific cancer types [38–40]. Integration of two prognosis-related pCRCSC miRNAs into a pCRCSC miRNA signature by risk score method, based on their expression and relative contribution, successfully categorized patients into high- and low-risk groups with

large differences in OS. Furthermore, risk stratification showed a pCRCSC miRNA-based classifier as a strong prognostic factor that complements clinicopathological features and MSI status, thereby indicating the function of pCRCSC-related miRNAs in predicting the survival of CRC patients. A limitation of our study was that we only used the TCGA dataset due to the unavailability of the expression data of miR-664b-3p and miR-200c in other public databases. Nevertheless, because TCGA is a reliable database and our study included more than 500 patients, miRNAs identified as specifically

expressed in CSCs can be used as promising biomarkers to predict the survival of cancer patients.

## CONCLUSIONS

We performed a comprehensive pCRCSC miRNA expression profile analysis and identified a novel pCRCSC-based miRNA signature that was intricately associated with the survival of patients with CRC. Further, the patients were categorized into high- and low-risk groups with substantially different clinical

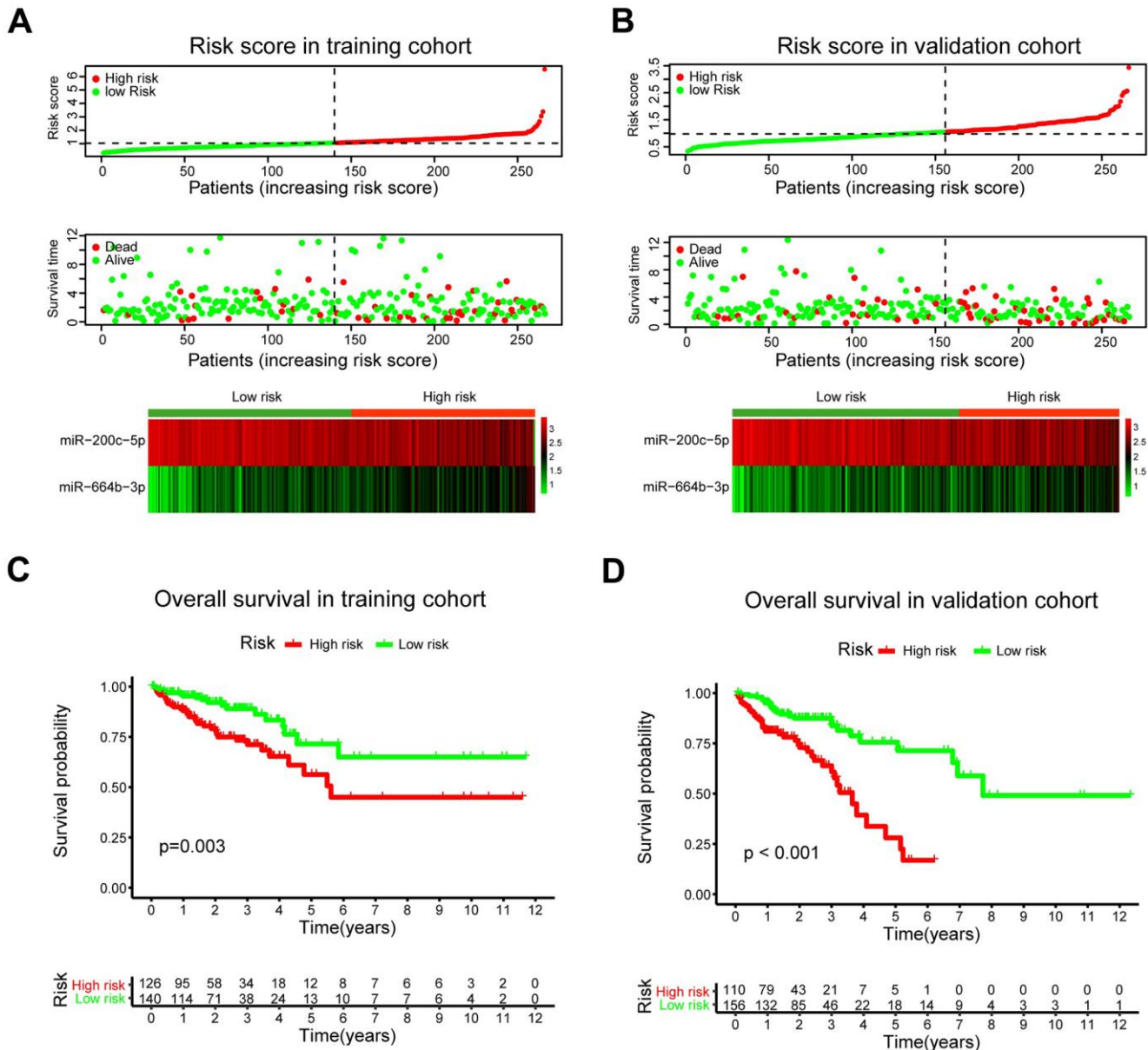
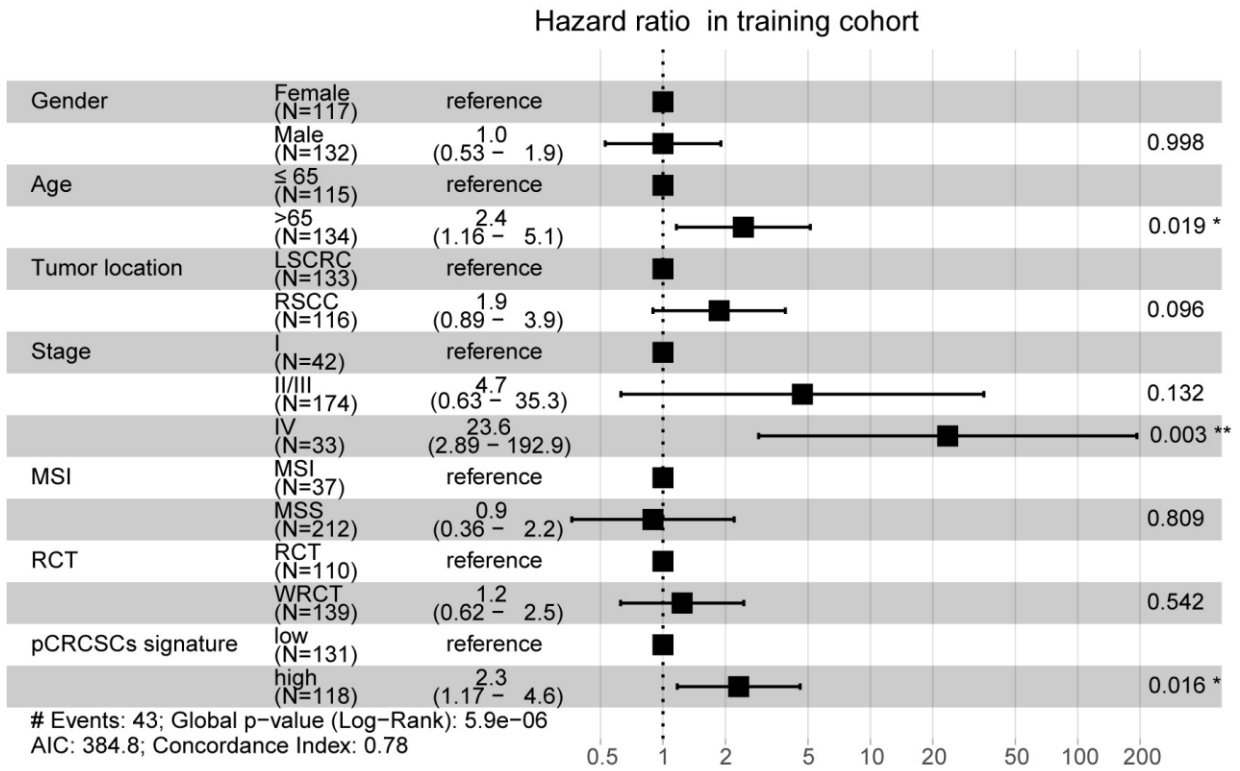


**Figure 5. A prognostic model based on pCRCSC-related miRNA signature stratifies the OS in CRC patients.** The distribution of risk score, overall survival (OS), OS status, and the heat map of prognostic pCRCSC miRNA signature in the training (A, B) validation cohorts. The dotted line indicates the cut-off point of the median risk score used to stratify the patients into low- and high-risk groups. Kaplan–Meier curves of OS for patients with CRC based on pCRCSC-related miRNA signature in the training (C, D) validation cohorts.



**A**



**B**

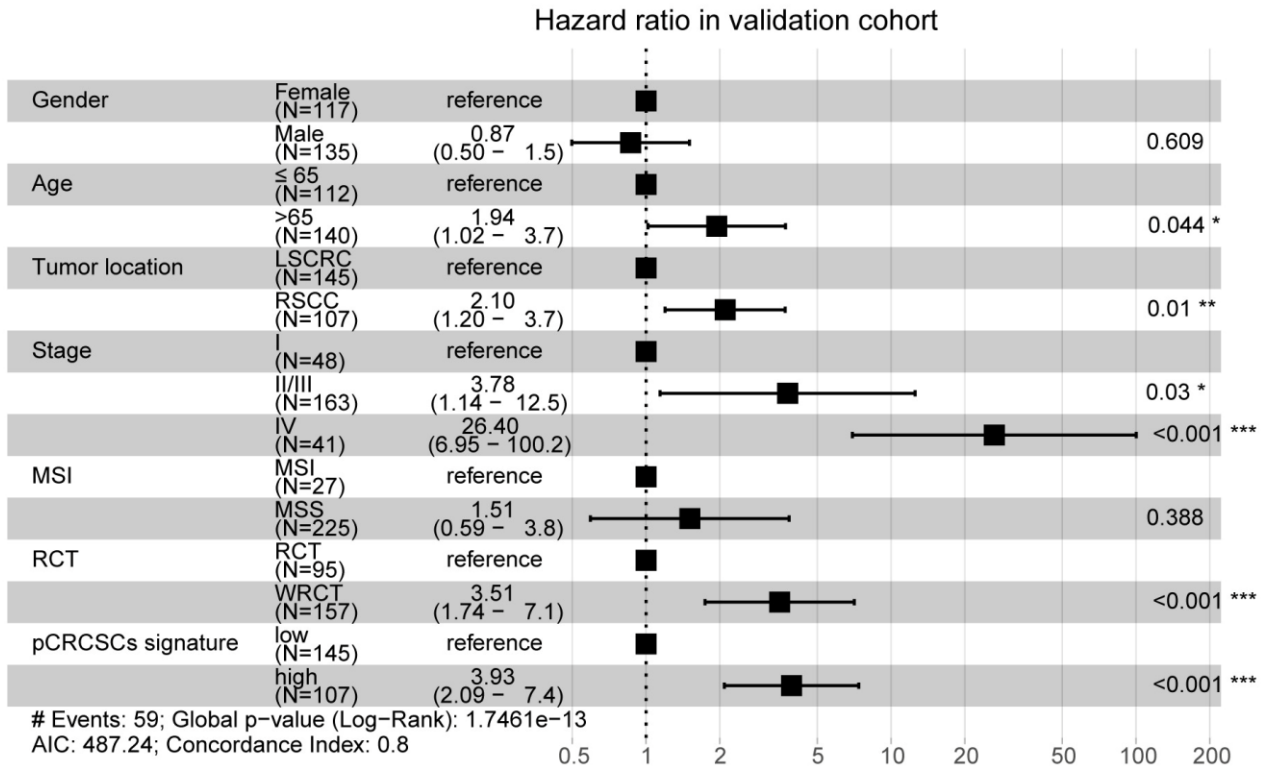


**Figure 6. pCRCSC-related miRNA signature is an independent prognostic factor for OS in CRC patients.** Forest plot summary of multivariate analyses for OS with gender, age, tumor location, tumor stage, MSI status, adjuvant chemoradiotherapy as covariates, and the risk based on pCRCSC-related miRNA signature in the training (A, B) validation cohorts. Squares on the transverse lines represent the hazard ratio (HR), whereas transverse lines represent 95% confidence interval (CI).

outcomes. Furthermore, the prognostic value of the pCRCSC-related miRNA signature was independent of other clinicopathological factors. Our study highlights the potential of pCRCSC-related miRNAs as alternative molecular markers, which could be used as promising therapeutic targets for CRC.

## MATERIALS AND METHODS

### Isolation, enrichment, and differentiation of CRCSC spheres from primary CRC

To isolate the primary CRCSC spheres, CRC samples were obtained from patients with primary colon adenocarcinoma who had undergone colon resection at the Department of Gastrointestinal Surgery, West China Hospital, Sichuan University. CRCSC spheres were isolated and expanded as described previously [3]. In brief, colon cancer tissues collected from surgical specimens were immediately minced on ice and suspended in the DMEM/F12 medium (HyClone, Logan, UT, USA). The tissue was mechanically and enzymatically dissociated, and the cell suspension was filtered. The dissociated single tumor cells were placed under stem cell conditions in serum-free DMEM/F12 medium supplemented with human recombinant EGF (PeproTech, Rocky Hill, NJ, USA) and bFGF (PeproTech) and cultured in ultra-low attachment plates (Corning, Corning, NY, USA). To obtain differentiated pCRCSCs, growth factors in the serum-free pCRCSC medium were removed and replaced with 20% FBS [3, 24].

### Xenograft experiments in a nude mouse model

Female nude mice (BALB/c strain, 4- to 6-week-old) were purchased from the Beijing Experimental Animal Centre of the Chinese Academy of Sciences (Beijing, China). The mice were housed under pathogen-free conditions, and the animal studies were performed according to the protocol approved by the Sichuan University Institutional Animal Care and Use Committee. The pCRCSC spheres and differentiated cells were trypsinized using 0.05% trypsin;  $5 \times 10^5$  cells were mixed with BD Matrigel (BD Biosciences, San Jose, CA, USA) at a 1:1 ratio and injected subcutaneously into the ventral wall of nude mice. Mice bearing the tumor were euthanized when the established criteria for the end-stage disease were reached, and the images were acquired.

### MiRNA isolation, miRNA microarray, and data analyses

MiRNAs of three pairs of CRCSCs and the corresponding differentiated cells were carefully isolated using “mirVana miRNA Isolation Kit” (Ambion,

Darmstadt, Germany) following the manufacturer’s instructions. The purity and concentrations of miRNA samples were measured and determined spectrophotometrically with NanoDrop ND-2000c (Thermo Fisher Scientific, Inc., Wilmington, DE, USA).

Genome-wide miRNA profiles of three pairs of CRCSCs and their corresponding differentiated cells were analyzed using Agilent Human miRNA Microarray (V21) at Shanghai Biotechnology Corporation (Shanghai, China). The differential expression of miRNAs was identified using the Limma package in R 3.6.0 and selected based on adjusted *p*-values ( $p < 0.05$ ). The absolute value of log<sub>2</sub> fold change was  $>1$ .

### Prediction of target genes of differential miRNAs

MiRNA target genes were identified using miRWalk 2.0 (<http://zmf.umm.uni-heidelberg.de/apps/zmf/mirwalk2/miRetsys-self.html>), TargetScan 7.1 (<http://www.targetscan.org>), and miRDB (<http://mirdb.org/miRDB/>, v4.0). The target genes were further reduced by selecting those commonly predicted by all three databases.

### Gene ontology (GO) and kyoto encyclopedia of genes and genomes (KEGG) analyses

Biological process, cell component, molecular function, and KEGG pathways were annotated in the following way: the list of potential target transcripts for each pCRCSC-related miRNA was uploaded to the Database for Annotation, Visualization and Integrated Discovery (DAVID) (<https://david.ncifcrf.gov>) for functional annotation. A GO term and pathway were selected if miRNAs were significant ( $p < 0.05$ ). The top 15 GO terms and pathways were visualized using the “ggplot2” package in R 3.6.0.

### pCRCSC-related miRNA-based prognostic model development

Level-3 data of miRNA-seq, mRNA-seq, including Illumina HiSeq and Illumina GA platforms, as well as the potential batch effects were removed using the “combat” function of “sva” package of R. The clinicopathological data of TCGA colorectal samples (COREAD) were obtained from UCSC Xena (<https://xenabrowser.net/hub/>). The adjuvant radiochemotherapeutic data were downloaded from GDC (<https://portal.gdc.cancer.gov/projects>). The TCGA colorectal samples were randomly divided into training and validation cohorts using the “caret” R package in R 3.6.0.

MiRNAs sharing both differential pCRCSC miRNAs and TCGA-COREAD miRNA datasets were considered

as predictive prognostic markers for survival comparison, with the lowest log-rank  $p < 0.05$ . The candidate prognostic miRNA signature was identified using the multivariate Cox proportional hazard regression survival model. The prognostic risk scores for each patient were calculated using the formula based on the coefficient from the multivariate Cox proportional hazard regression model. The optimal cut-off was automatically selected by the X-tile software version 3.6.1 (Yale University School of Medicine, New Haven, CT, USA). The patients were subsequently divided into high- and low-risk groups using the optimal cut-off. Next, the area under the curve (AUC) was applied to assess the predictive accuracy of the pCRCSC miRNA prognostic model using the “survival ROC” package in R 3.6.0.

The differences in OS between the high and low pCRCSC-related miRNA scores were analyzed using the Kaplan–Meier (K–M) curve with a log-rank test based on the “survival” package in R 3.6.0.

### Statistical analyses

We compared different clinicopathological parameters in low- and high-risk groups using the  $t$ -test for continuous variables and  $\chi^2$  test for categorical variables. The K–M method was used to compare the survival curves. The univariate and multivariate Cox regression model was used to study the prognostic significance of clinicopathological parameters and the CRCSC miRNA signature in the TCGA–COREAD data. All statistical tests were performed using the R software version 3.6.0. A  $p$ -value  $< 0.05$  was considered significant.

### Ethics statement

This study was approved by the Independent Ethics Committee of the West China Hospital of Sichuan University and was performed in accordance with the Declaration of Helsinki (1983). Informed consent was obtained from all patients who provided samples.

### Editorial note

<sup>&</sup>This corresponding author has a verified history of publications using a personal email address for correspondence.

### Abbreviations

miRNAs: microRNAs; CSCs: cancer stem cells; CRC: colorectal cancer; pCRCSCs: primary CSCs from CRC patients; GO: gene ontology; KEGG: Kyoto

Encyclopedia of Genes and Genomes; OS: overall survival.

### AUTHOR CONTRIBUTIONS

Conceptualization: C-W.F., Z-G.Z., H.Z., X-M.M., and X-F.S. Data curation: C-W.F., R.L., C.F., Z-Y.L., Y.L., Z-G.Z., H.Z., X-M.M., and X-F.S. Formal analysis: C-W.F., R.L., C.F., Z-Y.L., X-L.Z., and Y.L. Investigation: H.Z., X-M.M., and X-F.S. Methodology: C-W.F., R.L., X-L.Z., Z-Y.L., H.Z., X-M.M., and X-F.S. Project administration: Z-G.Z., H.Z., X-M.M., and X-F.S. Resources: Z-G.Z. and X-M.M. Software: C-W.F., R.L., C.F., and X-L.Z. Supervision: H.Z., X-M.M., and X-F.S. Validation: R.L., C.F., Z-Y.L., Y.L., Z-G.Z., X-M.M., and X-F.S. Visualization: C-W.F. and X-L.Z. Writing the original draft: C-W.F. and X-F.S. Writing, reviewing, and editing: R.L., C.F., X-L.Z., Z-Y.L., Y.L., Z-G.Z., H.Z., X-M.M., and X-F.S.

### ACKNOWLEDGMENTS

The authors are grateful to the Institutional Ethics Committee, Sichuan University, China, for approving the study. We also thank the participants and their families for their kind cooperation, generosity, and patience.

### CONFLICTS OF INTEREST

The authors declare that they have no conflicts of interest.

### FUNDING

This work was supported by grants from the Sichuan Science and Technology Program (No. 2017JY0061), Science Fund for Creative Research Groups of the National Natural Science Foundation of China (No. 81821002), and Swedish Cancer Foundation, Swedish Research Council, and Oncology Clinics in Linköping.

### REFERENCES

1. Siegel RL, Miller KD, Fedewa SA, Ahnen DJ, Meester RG, Barzi A, Jemal A. Colorectal cancer statistics, 2017. *CA Cancer J Clin.* 2017; 67:177–93. <https://doi.org/10.3322/caac.21395> PMID:28248415
2. Phi LT, Sari IN, Yang YG, Lee SH, Jun N, Kim KS, Lee YK, Kwon HY. Cancer Stem Cells (CSCs) in Drug Resistance and their Therapeutic Implications in Cancer Treatment. *Stem Cells Int.* 2018; 2018:5416923. <https://doi.org/10.1155/2018/5416923> PMID:29681949
3. Fan CW, Chen T, Shang YN, Gu YZ, Zhang SL, Lu R,

- OuYang SR, Zhou X, Li Y, Meng WT, Hu JK, Lu Y, Sun XF, et al. Cancer-initiating cells derived from human rectal adenocarcinoma tissues carry mesenchymal phenotypes and resist drug therapies. *Cell Death Dis.* 2013; 4:e828.  
<https://doi.org/10.1038/cddis.2013.337>  
PMID:[24091671](https://pubmed.ncbi.nlm.nih.gov/24091671/)
4. Shangguan W, Fan C, Chen X, Lu R, Liu Y, Li Y, Shang Y, Yin D, Zhang S, Huang Q, Li X, Meng W, Xu H, et al. Endothelium originated from colorectal cancer stem cells constitute cancer blood vessels. *Cancer Sci.* 2017; 108:1357–67.  
<https://doi.org/10.1111/cas.13262> PMID:[28421697](https://pubmed.ncbi.nlm.nih.gov/28421697/)
  5. Lu R, Fan C, Shangguan W, Liu Y, Li Y, Shang Y, Yin D, Zhang S, Huang Q, Li X, Meng W, Xu H, Zhou Z, et al. Neurons generated from carcinoma stem cells support cancer progression. *Signal Transduct Target Ther.* 2017; 2:16036.  
<https://doi.org/10.1038/sigtrans.2016.36>  
PMID:[29263908](https://pubmed.ncbi.nlm.nih.gov/29263908/)
  6. Pan C, Kumar C, Bohl S, Klingmueller U, Mann M. Comparative proteomic phenotyping of cell lines and primary cells to assess preservation of cell type-specific functions. *Mol Cell Proteomics.* 2009; 8:443–50.  
<https://doi.org/10.1074/mcp.M800258-MCP200>  
PMID:[18952599](https://pubmed.ncbi.nlm.nih.gov/18952599/)
  7. Mamoori A, Gopalan V, Smith RA, Lam AK. Modulatory roles of microRNAs in the regulation of different signalling pathways in large bowel cancer stem cells. *Biol Cell.* 2016; 108:51–64.  
<https://doi.org/10.1111/boc.201500062>  
PMID:[26712035](https://pubmed.ncbi.nlm.nih.gov/26712035/)
  8. Zhang R, Xu J, Zhao J, Bai J. Knockdown of miR-27a sensitizes colorectal cancer stem cells to TRAIL by promoting the formation of Apaf-1-caspase-9 complex. *Oncotarget.* 2017; 8:45213–23.  
<https://doi.org/10.18632/oncotarget.16779>  
PMID:[28423356](https://pubmed.ncbi.nlm.nih.gov/28423356/)
  9. De Robertis M, Mazza T, Fusilli C, Loiacono L, Poeta ML, Sanchez M, Massi E, Lamorte G, Diodoro MG, Pescarmona E, Signori E, Pesole G, Vescovi AL, et al. EphB2 stem-related and EphA2 progression-related miRNA-based networks in progressive stages of CRC evolution: clinical significance and potential miRNA drivers. *Mol Cancer.* 2018; 17:169.  
<https://doi.org/10.1186/s12943-018-0912-z>  
PMID:[30501625](https://pubmed.ncbi.nlm.nih.gov/30501625/)
  10. Sakaguchi M, Hisamori S, Oshima N, Sato F, Shimono Y, Sakai Y. miR-137 Regulates the Tumorigenicity of Colon Cancer Stem Cells through the Inhibition of DCLK1. *Mol Cancer Res.* 2016; 14:354–62.  
<https://doi.org/10.1158/1541-7786.MCR-15-0380>  
PMID:[26747706](https://pubmed.ncbi.nlm.nih.gov/26747706/)
  11. Wellner U, Schubert J, Burk UC, Schmalhofer O, Zhu F, Sonntag A, Waldvogel B, Vannier C, Darling D, zur Hausen A, Brunton VG, Morton J, Sansom O, et al. The EMT-activator ZEB1 promotes tumorigenicity by repressing stemness-inhibiting microRNAs. *Nat Cell Biol.* 2009; 11:1487–95.  
<https://doi.org/10.1038/ncb1998> PMID:[19935649](https://pubmed.ncbi.nlm.nih.gov/19935649/)
  12. Shi L, Xi J, Xu X, Peng B, Zhang B. MiR-148a suppressed cell invasion and migration via targeting WNT10b and modulating  $\beta$ -catenin signaling in cisplatin-resistant colorectal cancer cells. *Biomed Pharmacother.* 2019; 109:902–09.  
<https://doi.org/10.1016/j.biopha.2018.10.080>  
PMID:[30551544](https://pubmed.ncbi.nlm.nih.gov/30551544/)
  13. Jin Y, Wang M, Hu H, Huang Q, Chen Y, Wang G. Overcoming stemness and chemoresistance in colorectal cancer through miR-195-5p-modulated inhibition of notch signaling. *Int J Biol Macromol.* 2018; 117:445–53.  
<https://doi.org/10.1016/j.ijbiomac.2018.05.151>  
PMID:[29852230](https://pubmed.ncbi.nlm.nih.gov/29852230/)
  14. Ren D, Lin B, Zhang X, Peng Y, Ye Z, Ma Y, Liang Y, Cao L, Li X, Li R, Sun L, Liu Q, Wu J, et al. Maintenance of cancer stemness by miR-196b-5p contributes to chemoresistance of colorectal cancer cells via activating STAT3 signaling pathway. *Oncotarget.* 2017; 8:49807–23.  
<https://doi.org/10.18632/oncotarget.17971>  
PMID:[28591704](https://pubmed.ncbi.nlm.nih.gov/28591704/)
  15. Chen B, Zhang D, Kuai J, Cheng M, Fang X, Li G. Upregulation of miR-199a/b contributes to cisplatin resistance via Wnt/ $\beta$ -catenin-ABCG2 signaling pathway in ALDH1<sup>+</sup> colorectal cancer stem cells. *Tumour Biol.* 2017; 39:1010428317715155.  
<https://doi.org/10.1177/1010428317715155>  
PMID:[28639895](https://pubmed.ncbi.nlm.nih.gov/28639895/)
  16. Ju J. Implications of miRNAs in Colorectal Cancer Chemoresistance. *Int Drug Discov.* 2011; 2011:2063.  
PMID:[25750759](https://pubmed.ncbi.nlm.nih.gov/25750759/)
  17. Wang LQ, Yu P, Li B, Guo YH, Liang ZR, Zheng LL, Yang JH, Xu H, Liu S, Zheng LS, Zhou H, Qu LH. miR-372 and miR-373 enhance the stemness of colorectal cancer cells by repressing differentiation signaling pathways. *Mol Oncol.* 2018; 12:1949–64.  
<https://doi.org/10.1002/1878-0261.12376>  
PMID:[30171794](https://pubmed.ncbi.nlm.nih.gov/30171794/)
  18. Toden S, Kunitoshi S, Cardenas J, Gu J, Hutchins E, Van Keuren-Jensen K, Uetake H, Toiyama Y, Goel A. Cancer stem cell-associated miRNAs serve as prognostic biomarkers in colorectal cancer. *JCI Insight.* 2019; 4:e125294.  
<https://doi.org/10.1172/jci.insight.125294>  
PMID:[30895943](https://pubmed.ncbi.nlm.nih.gov/30895943/)

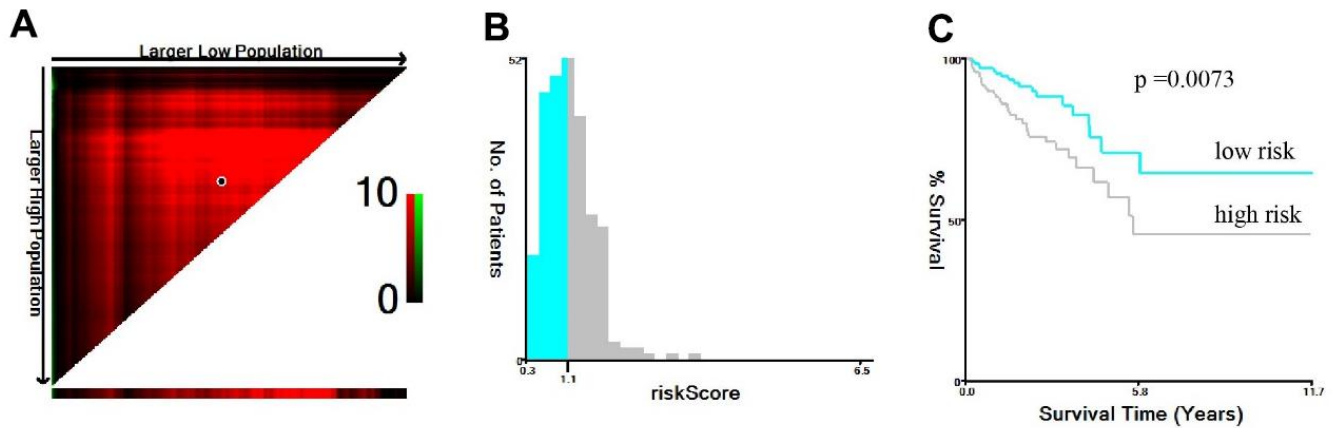


19. Asadzadeh Z, Mansoori B, Mohammadi A, Aghajani M, Haji-Asgarzadeh K, Safarzadeh E, Mokhtarzadeh A, Duijff PH, Baradaran B. microRNAs in cancer stem cells: Biology, pathways, and therapeutic opportunities. *J Cell Physiol.* 2019; 234:10002–17.  
<https://doi.org/10.1002/jcp.27885>  
PMID:[30537109](https://pubmed.ncbi.nlm.nih.gov/30537109/)
20. Khan AQ, Ahmed EI, Elareer NR, Junejo K, Steinhoff M, Uddin S. Role of miRNA-Regulated Cancer Stem Cells in the Pathogenesis of Human Malignancies. *Cells.* 2019; 8:840.  
<https://doi.org/10.3390/cells8080840> PMID:[31530793](https://pubmed.ncbi.nlm.nih.gov/31530793/)
21. Lou W, Liu J, Gao Y, Zhong G, Ding B, Xu L, Fan W. MicroRNA regulation of liver cancer stem cells. *Am J Cancer Res.* 2018; 8:1126–41.  
PMID:[30094089](https://pubmed.ncbi.nlm.nih.gov/30094089/)
22. Takebe N, Miele L, Harris PJ, Jeong W, Bando H, Kahn M, Yang SX, Ivy SP. Targeting Notch, Hedgehog, and Wnt pathways in cancer stem cells: clinical update. *Nat Rev Clin Oncol.* 2015; 12:445–64.  
<https://doi.org/10.1038/nrclinonc.2015.61>  
PMID:[25850553](https://pubmed.ncbi.nlm.nih.gov/25850553/)
23. Yang L, Shi P, Zhao G, Xu J, Peng W, Zhang J, Zhang G, Wang X, Dong Z, Chen F, Cui H. Targeting cancer stem cell pathways for cancer therapy. *Signal Transduct Target Ther.* 2020; 5:8.  
<https://doi.org/10.1038/s41392-020-0110-5>  
PMID:[32296030](https://pubmed.ncbi.nlm.nih.gov/32296030/)
24. Ricci-Vitiani L, Lombardi DG, Pilozzi E, Biffoni M, Todaro M, Peschle C, De Maria R. Identification and expansion of human colon-cancer-initiating cells. *Nature.* 2007; 445:111–15.  
<https://doi.org/10.1038/nature05384> PMID:[17122771](https://pubmed.ncbi.nlm.nih.gov/17122771/)
25. Hu Y, Fu L. Targeting cancer stem cells: A new therapy to cure cancer patients. *Am J Cancer Res.* 2012; 2:340–56.  
PMID:[22679565](https://pubmed.ncbi.nlm.nih.gov/22679565/)
26. Bertoli G, Cava C, Castiglioni I. MicroRNAs: New Biomarkers for Diagnosis, Prognosis, Therapy Prediction and Therapeutic Tools for Breast Cancer. *Theranostics.* 2015; 5:1122–43.  
<https://doi.org/10.7150/thno.11543> PMID:[26199650](https://pubmed.ncbi.nlm.nih.gov/26199650/)
27. Wu MJ, Kim MR, Chang CJ. Regulation of microRNA-200c in cancer stem cells. *Oncoscience.* 2015; 2:745–46.  
<https://doi.org/10.18632/oncoscience.204>  
PMID:[26501077](https://pubmed.ncbi.nlm.nih.gov/26501077/)
28. Shimono Y, Zabala M, Cho RW, Lobo N, Dalerba P, Qian D, Diehn M, Liu H, Panula SP, Chiao E, Dirbas FM, Somlo G, Pera RA, et al. Downregulation of miRNA-200c links breast cancer stem cells with normal stem cells. *Cell.* 2009; 138:592–603.  
<https://doi.org/10.1016/j.cell.2009.07.011>  
PMID:[19665978](https://pubmed.ncbi.nlm.nih.gov/19665978/)
29. Lin SS, Peng CY, Liao YW, Chou MY, Hsieh PL, Yu CC. miR-1246 Targets CCNG2 to Enhance Cancer Stemness and Chemoresistance in Oral Carcinomas. *Cancers (Basel).* 2018; 10:272.  
<https://doi.org/10.3390/cancers10080272>  
PMID:[30115848](https://pubmed.ncbi.nlm.nih.gov/30115848/)
30. Chen SM, Wang BY, Lee CH, Lee HT, Li JJ, Hong GC, Hung YC, Chien PJ, Chang CY, Hsu LS, Chang WW. Hinokitiol up-regulates miR-494-3p to suppress BMI1 expression and inhibits self-renewal of breast cancer stem/progenitor cells. *Oncotarget.* 2017; 8:76057–68.  
<https://doi.org/10.18632/oncotarget.18648>  
PMID:[29100291](https://pubmed.ncbi.nlm.nih.gov/29100291/)
31. Luo JL, Kamata H, Karin M. IKK/NF-kappaB signaling: balancing life and death--a new approach to cancer therapy. *J Clin Invest.* 2005; 115:2625–32.  
<https://doi.org/10.1172/JCI26322>  
PMID:[16200195](https://pubmed.ncbi.nlm.nih.gov/16200195/)
32. Stegh AH. Targeting the p53 signaling pathway in cancer therapy - the promises, challenges and perils. *Expert Opin Ther Targets.* 2012; 16:67–83.  
<https://doi.org/10.1517/14728222.2011.643299>  
PMID:[22239435](https://pubmed.ncbi.nlm.nih.gov/22239435/)
33. Tuttle TR, Mierzwa ML, Wells SI, Fox SR, Ben-Jonathan N. The cyclic GMP/protein kinase G pathway as a therapeutic target in head and neck squamous cell carcinoma. *Cancer Lett.* 2016; 370:279–85.  
<https://doi.org/10.1016/j.canlet.2015.10.024>  
PMID:[26551887](https://pubmed.ncbi.nlm.nih.gov/26551887/)
34. Fitzgerald TL, Lertpiriyapong K, Cocco L, Martelli AM, Libra M, Candido S, Montalto G, Cervello M, Steelman L, Abrams SL, McCubrey JA. Roles of EGFR and KRAS and their downstream signaling pathways in pancreatic cancer and pancreatic cancer stem cells. *Adv Biol Regul.* 2015; 59:65–81.  
<https://doi.org/10.1016/j.jbior.2015.06.003>  
PMID:[26257206](https://pubmed.ncbi.nlm.nih.gov/26257206/)
35. Prabhu VV, Allen JE, Hong B, Zhang S, Cheng H, El-Deiry WS. Therapeutic targeting of the p53 pathway in cancer stem cells. *Expert Opin Ther Targets.* 2012; 16:1161–74.  
<https://doi.org/10.1517/14728222.2012.726985>  
PMID:[22998602](https://pubmed.ncbi.nlm.nih.gov/22998602/)
36. Rinkenbaugh AL, Baldwin AS. The NF-κB Pathway and Cancer Stem Cells. *Cells.* 2016; 5:16.  
<https://doi.org/10.3390/cells5020016>  
PMID:[27058560](https://pubmed.ncbi.nlm.nih.gov/27058560/)
37. Matsui WH. Cancer stem cell signaling pathways. *Medicine (Baltimore).* 2016; 95:S8–19.  
<https://doi.org/10.1097/MD.0000000000004765>  
PMID:[27611937](https://pubmed.ncbi.nlm.nih.gov/27611937/)

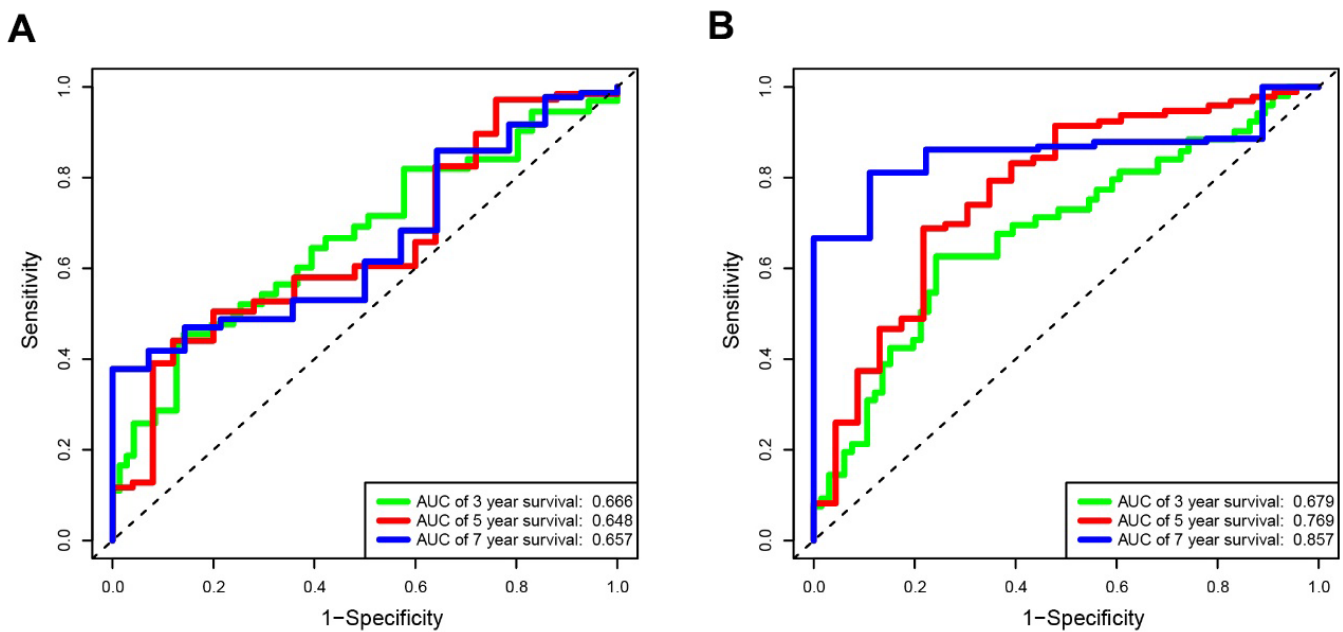
38. Diaz T, Tejero R, Moreno I, Ferrer G, Cordeiro A, Artells R, Navarro A, Hernandez R, Tapia G, Monzo M. Role of miR-200 family members in survival of colorectal cancer patients treated with fluoropyrimidines. *J Surg Oncol.* 2014; 109:676–83.  
<https://doi.org/10.1002/jso.23572>  
PMID:[24510588](https://pubmed.ncbi.nlm.nih.gov/24510588/)
39. Toiyama Y, Hur K, Tanaka K, Inoue Y, Kusunoki M, Boland CR, Goel A. Serum miR-200c is a novel prognostic and metastasis-predictive biomarker in patients with colorectal cancer. *Ann Surg.* 2014; 259:735–43.  
<https://doi.org/10.1097/SLA.0b013e3182a6909d>  
PMID:[23982750](https://pubmed.ncbi.nlm.nih.gov/23982750/)
40. Roh MS, Lee HW, Jung SB, Kim K, Lee EH, Park MI, Lee JS, Kim MS. Expression of miR-200c and its clinicopathological significance in patients with colorectal cancer. *Pathol Res Pract.* 2018; 214:350–55.  
<https://doi.org/10.1016/j.prp.2018.01.005>  
PMID:[29496312](https://pubmed.ncbi.nlm.nih.gov/29496312/)

SUPPLEMENTARY MATERIALS

Supplementary Figures



**Supplementary Figure 1. X-tile plots of pCRCSCs-related miRNAs signature for optimal cut-off determination in training cohort. (A, B)** The cut-off (IRS= 1.106) was optimized to separate low pCRCSCs-related miRNAs signature (blue) from high pCRCSCs-related miRNAs signature (gray) in the frequency histogram of training cohort. **(C)** Kaplan-Meier curve for testing the survival of sample subsets defined by optimized cutoff value of pCRCSCs-related miRNAs signature.



**Supplementary Figure 2. Time-dependent ROC curves for OS-specific pCRCSC-related miRNA signature. (A)** Time-dependent receiver operating characteristic curves at 3-, 5-, 7- years based on the pCRCSCs miRNAs signature in the training cohort. **(B)** Time-dependent receiver operating characteristic curves at 3-, 5-, 7- years based on the pCRCSCs miRNAs signature in the validation cohort.

## **Supplementary Tables**

Please browse Full Text version to see the data of Supplementary Tables 1–6, 8.

**Supplementary Table 1. Differentially expressed miRNAs between pCRCSCs and pCRCSC-derived differentiated cells.**

**Supplementary Table 2. Predictive target genes of pCRCSC-related miRNAs in different databases.**

**Supplementary Table 3. Differentially expressed miRNAs between normal and cancer tissues in patients from CRC from the TCGA dataset.**

**Supplementary Table 4. Differentially expressed mRNAs between normal and cancer tissues in patients with CRC from the TCGA dataset.**

**Supplementary Table 5. The integrated target genes of pCRCSC-related miRNAs using the database and TCGA miRNA–mRNA pairs.**

**Supplementary Table 6. GO analysis of target genes of pCSCSC-related miRNAs.**



**Supplementary Table 7. The KEGG pathway analysis of target genes of pCSCSC-related miRNAs.**

Term	Count	%	p value	Genes
hsa00030:Penose phosphate pathway	8	0.921659	8.55E-04	PGM2, GPI, RPE, PGM1, RPIA, PFKM, IDNK, PRPS1
hsa04520:Adherens junction	11	1.2672811	0.005685	PTPRJ, CDC42, SORBS1, BAIAP2, WASF2, MET, CTNND1, CDH1, WASL, INSR, TCF7L2
hsa04022:cGMP-PKG signaling pathway	18	2.0737327	0.006789	GNA13, KCNMA1, ATP1B3, PDE3A, ATP1A2, PPP1CB, VASP, KCNMB1, ATP2B1, EDNRB, ATP2B4, GNAQ, PLN, PDE5A, ADRA2A, INSR, MYLK, CALM1
hsa03040:Spliceosome	16	1.843318	0.006997	SRSF1, CHERP, SNRPB2, U2SURP, HNRNPU, SRSF3, HNRNPA3, SRSF2, SRSF5, TCERG1, SRSF7, SRSF6, SNRNP200, SNRPC, PRPF38B, RBM17
hsa04014:Ras signaling pathway	22	2.5345622	0.014486	FGFR2, PLD1, MET, KITLG, ARF6, KIT, FOXO4, STK4, CDC42, ETS2, RRAS2, GAB1, SOS2, PDGFRA, RALB, RAPIA, PDGFD, PRKACB, ABL1, INSR, GNG7, CALM1
hsa05200:Pathways in cancer	33	3.8018433	0.019088	GNA13, FGFR2, BID, E2F3, KITLG, FOXO1, EGLN1, CDH1, KIT, TCF7L2, PTEN, EDNRB, CDC42, BCL2, SOS2, RALB, TGFA, PRKACB, TPR, AXIN2, GNG7, PTGER4, EPAS1, MET, SKP2, ITGA2, FZD5, STK4, RAD51, HDAC2, GNAQ, PDGFRA, ABL1
hsa04152:AMPK signaling pathway	14	1.6129032	0.019246	PPP2R3A, PPP2R5A, FOXO1, ACACB, PFKM, PCK2, PPARGC1A, CPT1A, SLC2A4, PPP2CB, RAB14, RHEB, CAB39, INSR
hsa04972:Pancreatic secretion	11	1.2672811	0.03379	ATP2B1, KCNMA1, SLC26A3, CLCA1, ATP2B4, ATP1B3, SLC12A2, GNAQ, RAPIA, ATP1A2, SLC4A4
hsa04978:Mineral absorption	7	0.8064516	0.034055	SLC26A3, TRPM6, ATP1B3, SLC30A1, ATP1A2, SLC6A19, MT1G
hsa04931:Insulin resistance	12	1.3824885	0.037857	PPARA, SLC2A4, MLX, FOXO1, OGT, ACACB, PCK2, PTEN, PPARGC1A, INSR, PPP1CB, CPT1A
hsa04910:Insulin signaling pathway	14	1.6129032	0.043867	PRKAR2B, SORBS1, SLC2A4, SOS2, PHKA1, FOXO1, RHEB, PRKACB, ACACB, PCK2, PPARGC1A, INSR, PPP1CB, CALM1
hsa04261:Adrenergic signaling in cardiomyocytes	14	1.6129032	0.043867	PPP2R3A, ATP1B3, PPP2R5A, ATP1A2, PPP1CB, ATP2B1, ATP2B4, GNAQ, PLN, BCL2, PPP2CB, CAMK2D, PRKACB, CALM1
hsa04810:Regulation of actin cytoskeleton	19	2.1889401	0.045241	GNA13, FGFR2, ENAH, BAIAP2, PPP1R12B, WASF2, ITGA2, IQGAP2, PPP1CB, CDC42, DOCK1, EZR, CFL2, RRAS2, SOS2, PDGFRA, WASL, PDGFD, MYLK
hsa04922:Glucagon signaling pathway	11	1.2672811	0.048678	PPARA, GNAQ, PHKA1, CAMK2D, FOXO1, PRKACB, ACACB, PCK2, PPARGC1A, CPT1A, CALM1
hsa01212:Fatty acid metabolism	7	0.8064516	0.049232	ACOX1, ELOVL5, FADS1, HSD17B12, ACSL4, HADH, CPT1A
hsa01200:Carbon metabolism	12	1.3824885	0.049953	ME1, GPI, RPE, ME2, SUCLG2, ADPGK, RPIA, PFKM, IDNK, IDH3A, PC, PRPS1

**Supplementary Table 8. List of TCGA IDs for randomly grouped training and validation cohorts.**

**Supplementary Table 9. Univariate screening of pCRCSC-related miRNAs for OS in the training cohort.**

miRNAs	HR	HR.95L	HR.95H	p value
hsa-miR-142-3p	1.138066098	0.845905055	1.531134535	0.392881924
hsa-miR-182-5p	1.104825785	0.841234945	1.451009639	0.473486987
hsa-miR-183-5p	1.001026756	0.772377724	1.297363369	0.993811111
hsa-miR-196b-5p	0.879311673	0.729857866	1.059369303	0.175999667
hsa-miR-200c-5p	0.752123057	0.585874866	0.96554593	0.025412824
hsa-miR-223-3p	0.943087363	0.761021372	1.16871064	0.592357826
hsa-miR-338-3p	1.031115061	0.81146031	1.310228308	0.802055672
hsa-miR-338-5p	0.936520549	0.706315441	1.241755011	0.64864497
hsa-miR-345-5p	0.888078248	0.672958772	1.171963287	0.401630231
hsa-miR-3613-3p	1.135614061	0.730689762	1.764934125	0.571881692
hsa-miR-3614-5p	0.883264151	0.632935428	1.232598978	0.465361894
hsa-miR-3682-3p	1.18709029	0.769815217	1.830547545	0.437679937
hsa-miR-3940-3p	1.438622027	0.821532705	2.519234261	0.203279004
hsa-miR-4728-3p	1.061788613	0.716659991	1.573124038	0.764998501
hsa-miR-483-3p	0.896636456	0.764797104	1.0512029	0.17876179
hsa-miR-484	0.91859734	0.63191972	1.335329546	0.656421376
hsa-miR-5010-3p	1.100223917	0.656812919	1.842979384	0.716687824
hsa-miR-584-5p	0.83386517	0.679098374	1.023903382	0.082837655
hsa-miR-664b-3p	1.478618442	1.026965052	2.128906423	0.035462445
hsa-miR-664a-3p	1.106623781	0.731356495	1.674444955	0.631621212
hsa-miR-671-3p	0.96482922	0.658084789	1.41455241	0.854478312
hsa-miR-671-5p	1.086601465	0.761944892	1.549590733	0.646499192
hsa-miR-766-3p	0.931641917	0.643760078	1.348261087	0.707317911
hsa-miR-99b-5p	0.962351989	0.643240409	1.439774829	0.851897147
hsa-miR-494-3p	0.82117325	0.554024877	1.217139401	0.326458875
hsa-miR-598-3p	1.006536592	0.783515509	1.293038744	0.959340387

**Supplementary Table 10. Multivariate screening of pCRCSC-related miRNAs for OS in the training cohort.**

miRNA	coef	HR	HR.95L	HR.95H	p value
hsa-miR-200c-5p	-0.26960351	0.763682226	0.59521481	0.979832043	0.033990201
hsa-miR-664b-3p	0.383954209	1.468078215	1.003818613	2.147054873	0.047746837

**Supplementary Table 11. Univariate analysis of pCRCSC-related miRNA signature for OS in the training cohort.**

Parameters	HR	HR.95L	HR.95H	p value
Gender (Male vs Female)	1.409341027	0.767455353	2.588088183	0.268524673
Age ( $\leq 60$ vs $> 60$ )	2.530791757	1.275012442	5.023407384	0.00794166
Location (RSCC vs LSCRC)	1.129825063	0.617866334	2.065988392	0.6918184
pTNM (II/III vs I)	5.209048044	0.707243848	38.36609056	0.105238693
pTNM (IV vs I)	20.28084515	2.677647553	153.6097159	0.003575243
MSI (MSS vs MSI)	1.015366899	0.451256094	2.284667076	0.970599452
RCT (WRCT vs RCT)	0.906118362	0.495940318	1.655542925	0.748521717
risk (High vs low)	2.17329531	1.160487595	4.070024121	0.015311349

**Supplementary Table 12. Univariate analysis of pCRCSC-related miRNA signature for OS in the validation cohort.**

<b>Parameters</b>	<b>HR</b>	<b>HR.95L</b>	<b>HR.95H</b>	<b>p value</b>
Gender (Male vs Female)	1.074137693	0.639349115	1.804603707	0.787025435
Age ( $\leq 60$ vs $>60$ )	2.510383032	1.396271857	4.51346415	0.002103413
Location (RSCC vs LSCRC)	1.754334544	1.049870147	2.931495576	0.031893283
pTNM (II/III vs I)	2.971275024	0.910809589	9.692997719	0.071057644
pTNM (IV vs I)	12.36401574	3.657776016	41.79285021	5.19E-05
MSI (MSS vs MSI)	1.252524391	0.534756327	2.933705079	0.604101677
RCT (WRCT vs RCT)	1.251448747	0.733429318	2.1353441	0.410642781
risk (High vs low)	3.709875215	2.114370252	6.509349107	4.87E-06